Jurnal Teknologi

Full Paper

THE HELICAL SPRING PERFORMANCE OF STEEL BARS BY EXPERIMENTAL AND ANALYTICAL STUDIES

Erna Suryani[a,b], Ali Awaludin[a*], Inggar Septhia Irawati[a], Angga Fajar Setiawan[a], Henricus Priyosulistyo[a]

[a]Civil and Environmental Engineering, Universitas Gadjah Mada, Yogyakarta, Indonesia
[b]Civil Engineering, Politeknik Negeri Banyuwangi, Banyuwangi, Indonesia

Article history
Received
23 December 2024
Received in revised form
30 September 2025
Accepted
30 September 2025
Published Online
27 February 2026

*Corresponding author
ali.awaludin@ugm.ac.id

Graphical abstract

Specimen

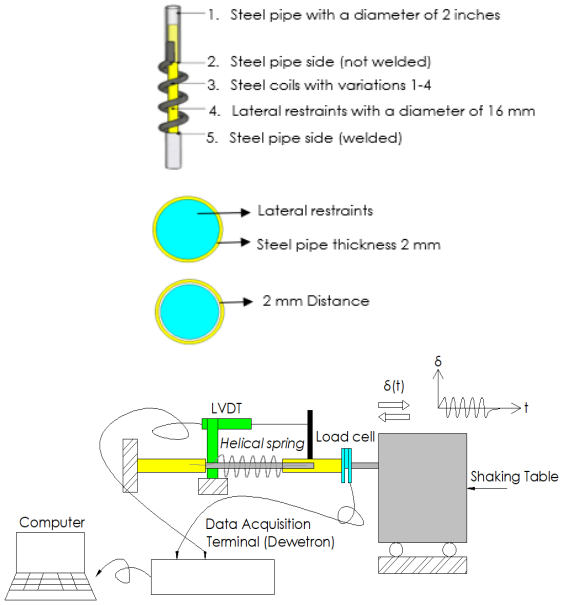

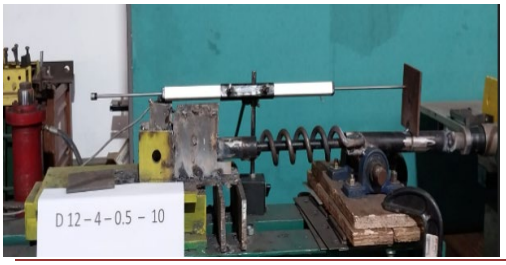

Abstract

The implementation effective mitigation strategies to improve the seismic performance of infrastructure is essential. Among these strategies is the use of local materials to reduce production costs while being easily obtained. An example of an energy dissipation device is the helical spring, which operates based on a yielding plastic deformation or displacement-controlled mechanism. Therefore, this study aimed to determine the strength, stiffness, and damping ratio of a helical spring. The methods used included experimental testing in the laboratory as well as analytical calculations based on spring mechanics theory, respectively. During this analysis, experimental testing was conducted to obtain values for the damping ratio, effective stiffness, strength, and displacement when the helical spring yielded, and the results were compared with analytical calculations. The material used was locally produced steel bars with diameters ranging from 6 - 19 mm and numbers of coils from 1 - 4. The testing was conducted in a laboratory using a shaking table with a frequency of 0.5 Hz. The results showed that the damping values were relatively similar for all variations of the helical spring. However, the resulting damping values were lower with an increase in the number of coils. As the diameter of steel bars in the helical spring increased, the yield strength also rose, leading to greater effective stiffness. Significant differences were observed in experimental and analytical results for steel bars with larger diameters. The results showed that the helical spring could be used as a passive energy dissipation device for low-rise lightweight structures.

Keywords: Dissipation devices, coils, steel bars, helical spring, shaking table

1.0 INTRODUCTION

Seismic activity is posing significant risks as it requires building engineers to create effective strategies that improve structural resilience. Advances in earthquake engineering help reduce the impact of seismic events. These advances focus on following code standards to lower the risk of failure and loss [1,2,3]. Indonesia encounters a high risk of earthquakes because the country is situated in the Pacific Ring of Fire. Therefore, buildings should meet code standards and include energy dissipation devices to minimize risks. Devices such as seismic dampers, seismic isolators, and flexible connections can lessen the effects of seismic forces on structures. However, the development of cost-effective energy dissipation devices is particularly needed for low-rise lightweight structures. The strategy includes using local materials to cut production costs while ensuring availability. Unfortunately, current energy dissipation study targets high-rise buildings. Consequently, the devices created are often too expensive for low-rise lightweight structure applications. There is limited study on affordable energy dissipation devices for low-rise lightweight structures that use simple manufacturing processes. Installing these devices is crucial for building earthquake-resistant structures. This method is part of earthquake protection systems, as shown in Figure 1.

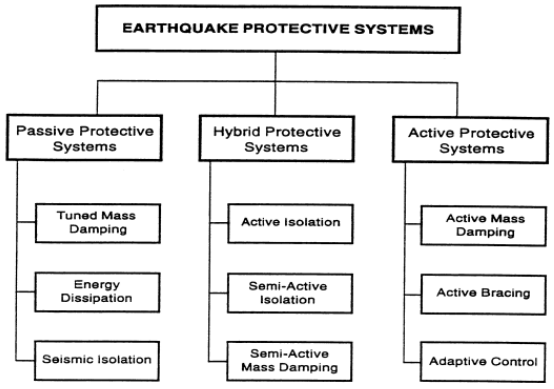

Figure 1 Earthquake protective systems [4]

Metallic, friction, viscoelastic solid, viscoelastic or viscous fluid, tuned mass, and tuned liquid are the types of dampers that belong to passive energy dissipation. Passive energy dissipators can be simply categorized into two types, namely hysteretic and viscoelastic. Moreover, hysteretic dissipators include metal yielding by flexure, shear, torsion, extrusion (metallic dampers), and sliding (frictional dampers) as these mechanisms are primarily displacement-dependent. Viscoelastic systems consist of viscoelastic solids, fluid orifices (fluid dampers), and viscoelastic fluids [4].

Study related to energy dissipation devices is currently focused on development for high-rise buildings, such as tuned mass dampers (TMD). Research on the behavior of multidirectional box-shaped shear dampers (MBSD), which consist of box-shaped steel plates made from hot-rolled steel coils (SPHC), shows that MBSD can achieve sufficient shear strength and energy dissipation in various load directions [5]. Another study on the types of Slit Steel Damper (SSD), Tapered Steel Damper (TSD), and Oval Steel Damper (OSD) concerning damping capacity and effective stiffness using cyclic loading signified that all three types of dampers have relatively similar energy damping capacity. There are differences in stress and strain distribution, while the SSD damper has the highest effective stiffness compared to TSD and OSD [6]. This is similar to a study on steel frames reinforced with SSD, which showed a 12% increase compared to steel frames without SSD dampers [7]. Another study on Multiple Tuned Mass Dampers (MTMDs) in reducing the dynamic response of multi-story frame structures equipped with viscous damping systems made of Thermoplastic Polyurethane (TPU) could effectively reduce the dynamic response of multi-story frame structures to dynamic loads [8]. In addition, similar results on a type of TMD, the pendulum-tuned mass damper, for reducing wind turbine vibrations, showed effectiveness in reducing vibration response by up to 12% [9]. The use of active TMD and Semi-Active Tuned Mass Dampers (SATMD) in high-rise buildings has shown effectiveness in reducing vibration response [10,11], and even the installation of TMD at optimal positions can reduce acceleration and displacement by up to 50% [12]. Considering the development of these studies, the analysis of passive energy dissipation devices for low-rise lightweight structures using local materials is still limited. Meanwhile, a study of factory-produced viscous dampers with a strength of 4 kN installed in inter-story and cross-story models for low-rise lightweight structures showed effective results in reducing the drift of two-story timber houses compared to houses without dampers [13]. Based on these conditions, helical springs are selected as an alternative passive energy dissipation device for application in low-rise lightweight structures. The element, as a dissipation device, works based on a yielding mechanism through plastic deformation.

A helical spring is a mechanical component made from coiled wire formed into a spiral shape with a constant pitch. The combined component is available in two distinct geometric configurations, cylindrical and rectangular. It can show open or closed coil types, depending on the orientation angle relative to the vertical axis. The geometric design of helical springs using metaheuristic optimization with compression loading signifies effective results in the helical spring design process [14]. Additionally, the design of the element using programming compared to spring mechanics theory, with a diameter of 6 mm, finds that this computational system provides consistent results [15]. Helical spring with rectangular shape, fixed diameter, and specific number of coils

has been shown through compression testing to withstand greater loads [16]. In addition to testing using compression methods, a study on the element with tensile testing was conducted through 3D printing using one type of diameter and number of coils. This study showed the importance of considering the nonlinear geometric effects when predicting the tensile performance of helical springs [17]. Various numerical and experimental methods have been used to improve the strength and mechanical reliability of the element, particularly through material selection. Several studies have shown that using different materials, such as carbon steel, alloy steel, synthetic resin, and composites, has a significant impact on the mechanical performance as well as durability of springs. Differences in material properties and production conditions across regions have led to varied performance outcomes in these results [18,19, 20,21,22]. Studies have investigated the use of helical springs for seismic resistance in buildings concerning industrial applications. This innovation includes the incorporation of a TMD equipped with a super elastic helical spring made of shape memory alloy (SMA). The system has been proven to improve passive energy dissipation and significantly reduce structural vibration responses, indicating the potential of SMA-based helical springs in civil engineering and disaster mitigation applications [23,24].

Previous studies had shown limitations in varying the diameter and number of coils of helical spring, limiting a comprehensive understanding of spring characteristics in various geometries. To overcome these limitations, this study used steel bar diameters between 6 and 19 mm as well as the number of coils between 1 and 4. Different from previous methods that used compression and tensile testing methods, this study used a shaking table to evaluate the performance of helical springs (strength, stiffness, and damping ratio) to be compared with analytical calculations based on spring mechanics theory. In addition to geometric aspects and testing methods, this study applied locally sourced steel bars to increase practical relevance and support applying local material-based technology in construction. Steel cylinder guide bars at the helical spring controlled lateral movement and minimized rotation or tilting during testing.

This study contributes to current knowledge concerning the influence of geometric parameters, particularly spring diameter and number of coils, on developing passive energy dissipation devices in helical spring systems. Moreover, this result provides an improved comprehension of spring behaviour in different configurations concerning strength, stiffness, and damping.

2.0 METHODOLOGY

The objective of this study on helical springs was to evaluate the characteristics of various steel bar diameters through experimental testing and analytical results. This study focused on investigating stiffness, strength, and energy dissipation capacity. The steps used during the analysis were as follows:

a. Experimental procedure began with tensile testing of steel bars to determine the yield and tensile strengths. These mechanical properties were then used as input parameters for analytical calculations based on spring mechanics theory.
b. Fabrication of helical spring test specimens. The helical spring was tested using a shaking table to produce hysteresis curves that reflected energy dissipation capabilities.
c. After testing the helical spring, analytical calculations based on spring mechanics equations were performed to determine the relevant mechanical parameters.
d. Experimental results were then compared with analytical outcomes to evaluate both methods.

2.1 Materials and Specimens

Steel bars with diameters of 6 mm, 8 mm, 10 mm, 12 mm, 16 mm, and 19 mm were used to form the helical spring. Steel bars are locally produced in Indonesia and formed into helical springs. The helical spring was said to be a spiral spring made with different numbers of coils. The number of coils used was 1-4 coils, while the outer diameter of each helical spring was 2 inches. Moreover, several major parameters influenced the strength and performance of helical springs, particularly geometric configuration as well as material properties. The geometric parameters included the diameter of the steel bar (d), the diameter of the coil (D), the number of coils (n), and the yield strength of the steel bar (f_y). Figures 2 and 3 show these parameters as well as the detailed configuration of the helical spring.

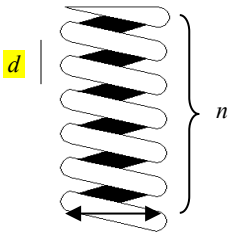

Figure 2 Parts of the helical spring

2.2 Method

The methods used in this study included analytical studies of helical springs and laboratory testing. Tests conducted in the laboratory included tensile testing of steel bars and testing of helical springs.

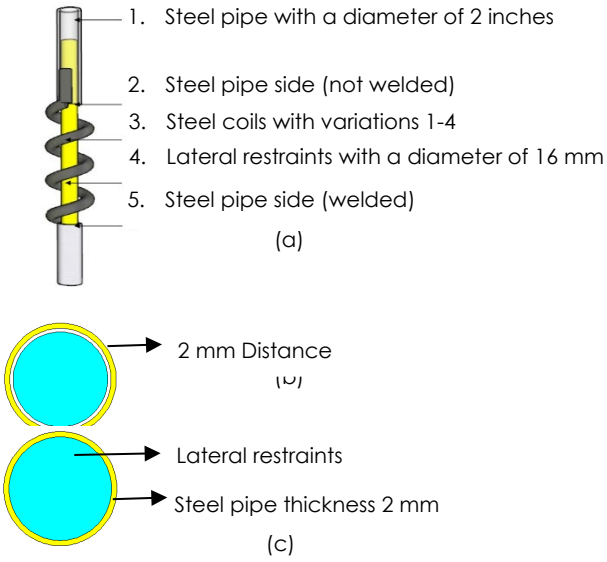

Figure 3 Detailed of helical spring (a) Helical Spring part, (b) Top view part 2, (c) Top view part 5

2.2.1 Analytical Studies of Helical Spring

The equations used in the analysis calculations were based on Richard G Budynas and J. Keith Nisbett's "Mechanical Engineering Design" textbook and R. Khurmi and J. Gai's "Machine Design" textbook on spring mechanics theory. Spring mechanics theory included several aspects, such as spring index, deflection behaviour, and the strength of helical springs in resisting loads. Furthermore, the fundamental equations derived and presented in this study provided the theoretical foundation for the analytical calculations, particularly in evaluating the deformation characteristics and yield strength limits of the springs under loading. The steps in analysing the strength of helical spring after the parameters *d*, *D*, *n*, and f_y were determined were as follows [15,25,26]:

a) Calculating Spring Index C.
This was the proportion of wire diameter to coil mean diameter. The spring index was determined by dividing the outer diameter D by the diameter of the spring steel bar *d*, as described in Equation 1.

$$C = \frac{D}{d} \quad (1)$$

b) Calculating the shear stress correction factor value K.
The correction factor used in calculating the maximum shear stress in a helical spring, known as the shear stress correction factor or Wahl factor, adjusts the theoretical shear stress. This considers the effects of spring coil geometry and stress concentration that were not considered in the basic formula. The correction factor for shear stress in spring was calculated using Equation 2.

$$K = 1 + \frac{1}{2C} = \frac{2C + 1}{2C} \quad (2)$$

c) Calculating the load at the yield point, F
The yield load of spring was the maximum load that it could withstand before the material began to experience plastic or permanent deformation. The load F that the spring could sustain until it reached the yield point was determined using Equation 4.

$$F = \frac{\tau \times \pi \times d^3}{8 \times K \times D} \quad (3)$$

Where:
τ = Shear stress

d) The yield deformation of spring was the permanent deformation that occurred when the load exceeded the yield strength of spring material. Calculating the yield deformation y was conducted using Equation 5.

$$y = \frac{8 \times F \times n \times D^3}{d^4 \times G} \quad (4)$$

e) G was the shear modulus, as the shear modulus described the magnitude of the shear stress required to produce a given amount of shear deformation. This process was calculated by using Equation 6 during the analysis.

$$G = \frac{E}{2 \times (1 + \nu)} \quad (5)$$

Where: E = Modulus of Elasticity
ν = Poisson's Ratio

2.2.2 Tensile Testing

Material testing was used to obtain the yield and tensile strength values of reinforcing steel bars with diameters of 6, 8, 10, 12, 16, as well as 19 mm, which were essential for validating the helical spring data analysis. This testing used a Universal Testing Machine (UTM) with a capacity of 1000 kN and a loading speed of 2 kN/second. From the testing, values for yield point, strain, and modulus of elasticity were obtained. The stress-strain graph from the tensile test signified the yield strength, strain, elongation, and modulus of elasticity for the 6 mm diameter steel bars. Table 1 shows the average yield strength (f_y), tensile strength (f_u), strain, elongation, and modulus of elasticity values for each steel bar diameter tested.

2.2.3 Testing of Helical Spring

Helical spring tests were conducted using steel bars of various diameters, specifically diameters of 6, 8, 10, 12, 16, and 19 mm, with coil counts ranging from 1 to 4, as well as a constant inner coil diameter of 2 inches. The number of test specimens used during the analysis was one for each test variation. Table 2 shows the variations in specimen configurations during the process.

Table 1 Yield Strength, Tensile Strength, Strain, Elongation, and Modulus of Elasticity Values

Dia.	Elongation (%)	Strain (ε)	MOE (E, MPa)	Yield Strength (f_y, MPa)	Tensile Strength (f_u, MPa)
6	16%	0.002	214607	510.79	671.01
8	14%	0.002	211394	496.17	701.17
10	16%	0.002	193335	448.64	619.12
12	20%	0.002	221091	410.06	553.54
16	20%	0.002	193162	429.25	623.37
19	20%	0.002	232949	442.01	642.68

Testing was performed dynamically 1.25 m by 1.25 m shaking table equipped with a load cell capacity of 1000 kN. An LVDT was positioned on the helical spring with a 30 cm length capacity. The load was applied using displacement control at a frequency of 0.5 Hz to determine the achievement of energy dissipation. This frequency represented low earthquake frequencies based on the ratio of ground acceleration to ground velocity (A/V) [27]. Figure 2 and 4 showed the helical spring details as well as the helical spring test setup. Loading was applied using displacement control for testing helical spring on the shaking table based on the target yield displacement of each spring as calculated from theoretical Equations 1 to 6. The displacement controls included a series of values before yield displacement, up to three times yield displacement. This had target displacements of 4, 6, 8, 10, 20, 30, 40, 50, and 60 mm, as shown in Figure 5. For lower yield points, displacements were applied in single-millimeter intervals from 1 to 10 mm. Moreover, displacement-controlled loading was performed on seven cycles, consisting of two preliminary series followed by five main sequences, all based on the target displacement. The yield point for each steel bar helical spring was determined using a method proposed by Park [28]. This point was identified from the load-displacement curve, based on the first yield point where the curve gradient change signified inelastic conditions, as shown in Figure 6.

The energy dissipation value produced was represented by the area formed when cyclic loading occurred between load and displacement. The magnitude of energy dissipation in each cycle showed the capacity of the structure' to absorb and dampen the external loads.

The system damping in the i-th cycle was expressed as the Equivalent Viscous Damping Ratio (EVDR), which was calculated by analyzing the hysteretic curve from dynamic testing results [29]. During the analysis, the ratio (ξ_{eq}) was determined by examining the hysteretic curve from dynamic testing results. ξ_{eq} was expressed as the magnitude of the comparison between the energy lost and stored in a cycle. Moreover, the ratio (ξ_{eq}) value was calculated using Equation 6, where E_i represented the amount of energy loss, and E_{si} was the maximum energy that could be stored (Equation 7). The magnitude of E_i was equivalent to the area of the hysteretic loop, while E_{si} represented half the area of the triangle formed by Δ_i and Q_i. Where Δ_i was the maximum displacement, and Q_i represented the maximum force. Helical spring test results used for further analysis with a linear dynamic procedure, required an effective stiffness value that was calculated using Equation 9.

$$\xi_{eq} = \frac{E_i}{4 \times \pi \times E_{si}} \quad (6)$$

$$E_{si} = \frac{Q_i \times \Delta_i}{2} \quad (7)$$

$$K_{eff} = \frac{|F_{max}|+|F_{min}|}{|\delta_{max}|+|\delta_{min}|} \quad (8)$$

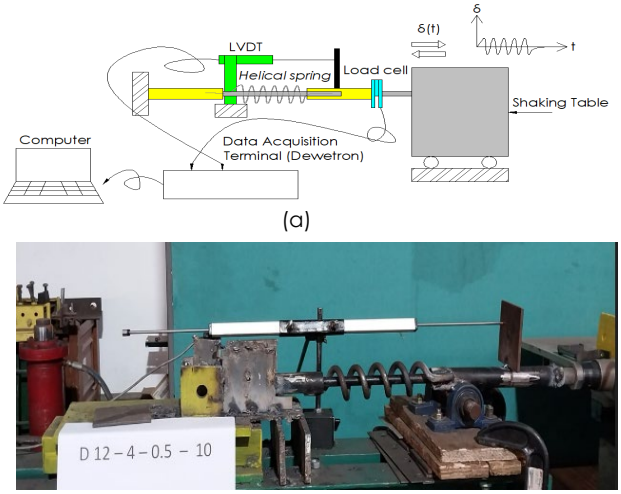

(a)

(b)

Figure 4 The Testing of the helical spring device on the shaking table (a) Testing scheme of helical spring, (b) Testing photos in the Laboratory

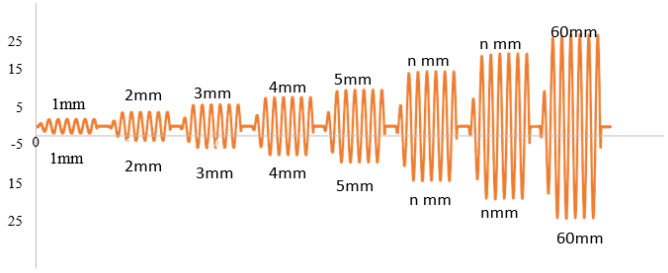

Figure 5 The displacement control of the test

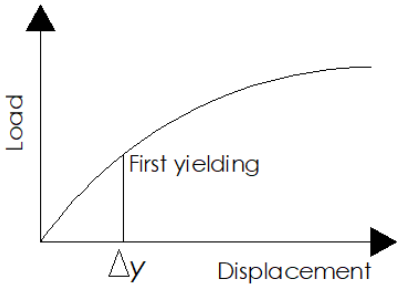

Figure 6 Yield point determination [28]

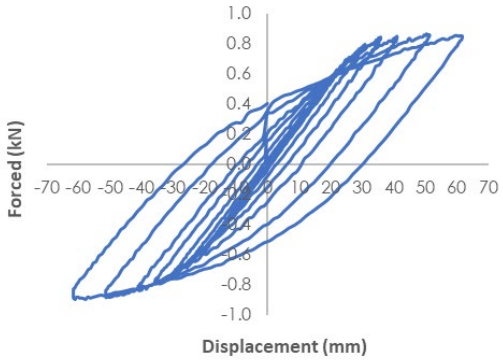

Figure 7 Hysteretic curve of helical spring d8-3 coils

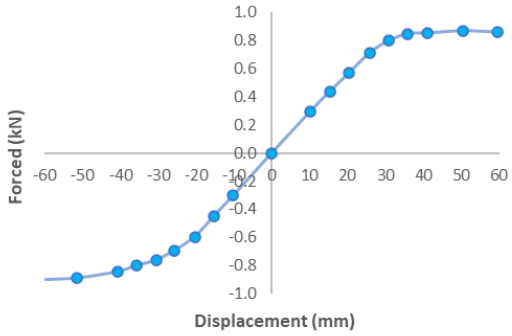

Figure 8 Skeleton curve of helical spring d8-3 coils

3.0 RESULTS AND DISCUSSION

3.1 Yield Strength and Yield Displacement of Helical Spring

Testing using a shaking table on each helical spring was used to obtain stiffness and strength values, including yield strength and displacement. These values were obtained from the hysteresis curve of the test, which was used to obtain the skeleton curve and damping value in each test. From the skeleton curves, the yield strength and displacement values were obtained for each steel-bar diameter and number of coils. Figure 7 shows a hysteresis curve for an 8 mm diameter steel bar with three coils, while Figure 8 shows the corresponding skeleton curve.

The strength and displacement values at the point of yielding for the helical spring with 8 mm diameter steel bar with three coils were shown in Figure 8. For skeleton curves of other helical spring variations, the test results with different steel bar diameters and coil counts were shown in Figures 9 to 14. The skeleton curves showed differences due to variations in the number of coils and coil diameter derived from testing each coil spring. The test results showed that the number of coils significantly affected the skeleton curve combined with different diameters. Based on Figures 9 to 14, large-diameter bars had greater strength. For instance, the yield strength value was 0.27 kN with a steel bar diameter of 6 mm and a single coil. Meanwhile, the outcome led to a 96% increase in yield strength, from 0.27 to 7.5 kN with 19 mm diameter and the same number of coils. Following this discussion, a similar trend was observed for four coils. The strength was 0.34 kN for a 6 mm diameter, increasing to 8 kN at 19 mm, which represented a 96% increase.

Table 2 Variations of helical spring test specimens

No	Steel bar diameter (mm)	Number of coils
1	6	1
2		2
3		3
4		4
5	8	1
6		2
7		3
8		4
9	10	1
10		2
11		3
12		4
13	12	1
14		2
15		3
16		4
17	16	1
18		2
19		3
20		4
21	19	1
22		2
23		3
24		4

The displacement test results further showed that as the steel bar diameter increased, the yield displacement decreased. Comparing the diameters of 6 and 19 mm with one coil, there was a 43% reduction in yield displacement. Based on the strength values obtained from the skeleton curve, this damper can be used for low-rise lightweight structures, similar to those studied in the previous viscous elastic damper study. Dampers with a force of 4 kN are used for low-rise lightweight structures in two-story timber houses [13].

3.2 Effective Stiffness and Damping Ratio of Helical Spring

Figures 15 -20 show the effective stiffness of the helical spring during the analysis. The effective stiffness value increased by 98.1%, from 0.021 to 1.12, for a spring count of one between diameters 6 and 19 mm. An increase of 98.3% from 0.014 to 0.826 was observed for coil count two. Moreover, there was an increase of 97.9% from 0.011 to 0.529 with three coils. The increase was 94.4%, from 0.011 to 0.185 for the four coils. The effective stiffness increased with the diameter of the steel bars but decreased as the number of coils multiplied. This signified that springs with fewer coils had higher effective stiffness.

Figures 21 to 26 show the damping value (EVER) for each helical spring based on the hysteresis curve. For the same displacement, damping values decreased as the number of coils increased. This was because additional coils reduced the amount of absorbed energy. The number of coils provided a significant role in the damping value for each diameter. Furthermore, concerning steel bars with diameters from 6-19 mm, the damping value ranged from 37 - 29% (one coil), 25 - 37% (two coils), 20 - 32% (three coils), and 15 - 28% (four coils), respectively. Different from previous results [14,16,17,18,20] that used experimental testing methods with static compression and tensile procedures, this study applied a shaking table test. This examination simulated dynamic loads more representative of actual conditions in the field during an earthquake, where the structure was subjected to repetitive loads. Consequently, the method offered advantages in evaluating the dynamic response of helical springs in a more realistic and applicable earthquake performance context. The results of this study on small test object diameters showed only a slight difference in values compared to previous study results using similar diameters with different numbers of coils [15].

3.3 Analytical and Experimental Comparison

The strength analysis of the helical spring, based on Equations 1 to 5, was shown in Table 3. These values were then used to validate the helical spring test results obtained from the shaking table experiments. Figures 27-30 showed a comparison between analytical results and experimental data on the yield strength for different numbers of coils as well as steel bar diameters. The maximum percentage difference between analytical and experimental results at 16 mm diameter was 35% for specimens with a single coil, while the minimum difference at 8 mm diameter was 2%. In the specimen with two coils, the largest difference occurred at a diameter of 16 mm, with a value of 45%. On the other hand, the lowest value of 0.63% was found at 8 mm. Concerning the specimen with three coils, the largest difference at a diameter of 16 mm was 35%, and the smallest difference of 0.87% was observed at 8 mm. The maximum percentage difference between experimental and analytical results for the specimen with four coils was found at 10 mm diameter of 107%, and the minimum difference of 0.58% occurred at 6 mm.

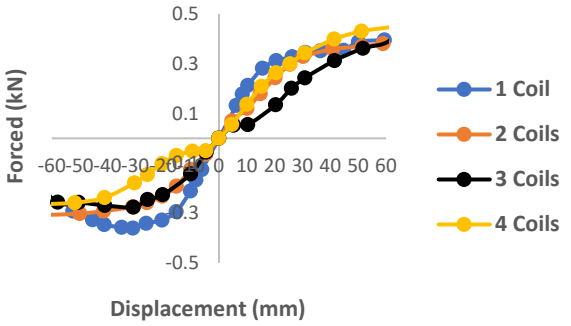

Figure 9 Skeleton curve d 6

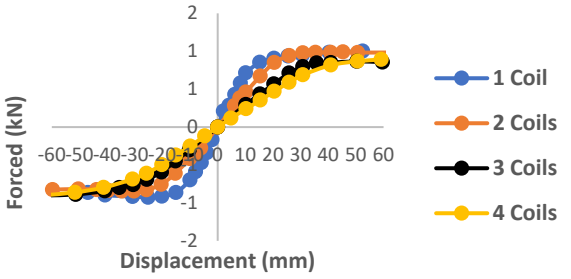

Figure 10 Skeleton curve d 8

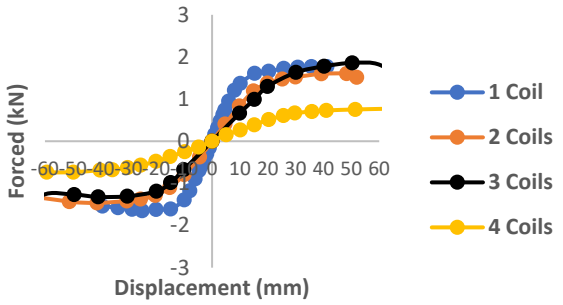

Figure 11 Skeleton curve d 10

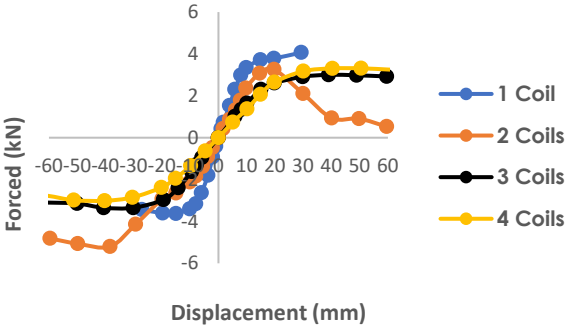

Figure 12 Skeleton curve d 12

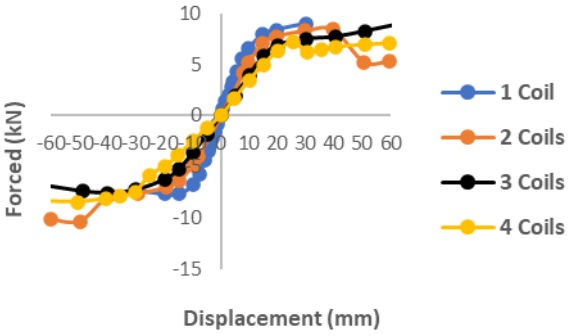

Figure 13 Skeleton curve d 16

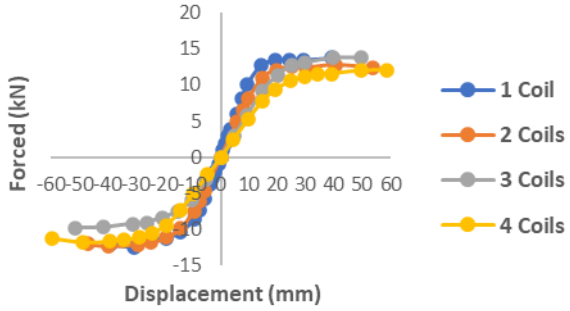

Figure 14 Skeleton curve d 19

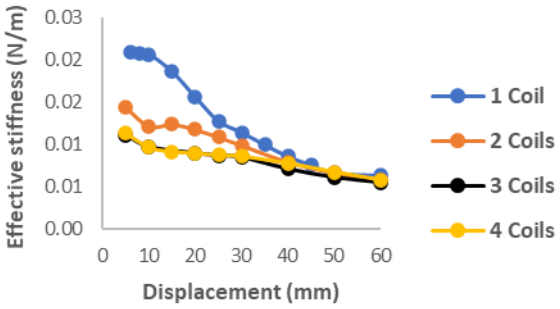

Figure 15 Effective stiffness d 6

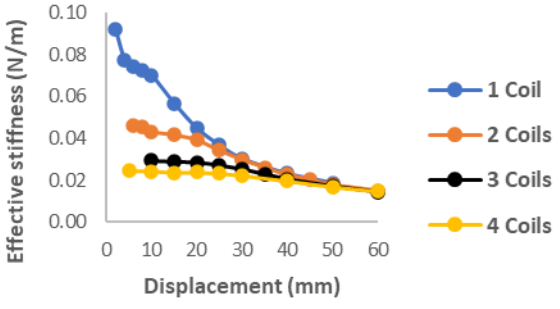

Figure 16 Effective stiffness d 8

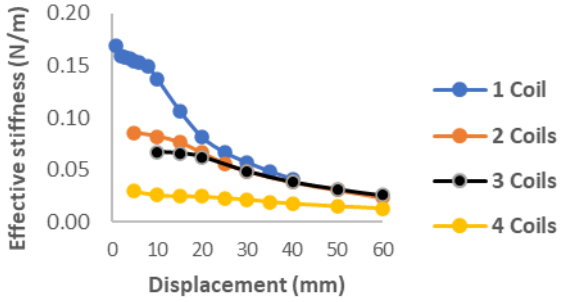

Figure 17 Effective stiffness d 10

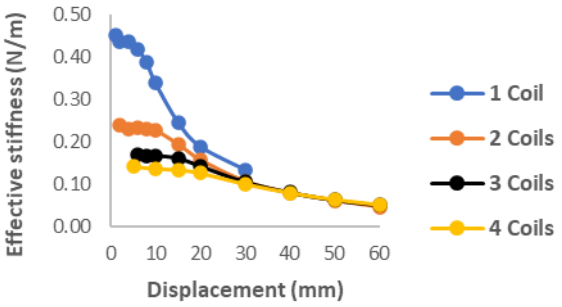

Figure 18 Effective stiffness d 12

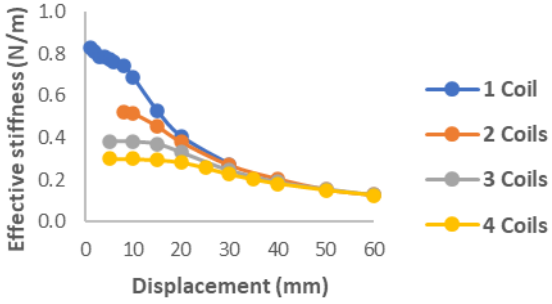

Figure 19 Effective stiffness d 16

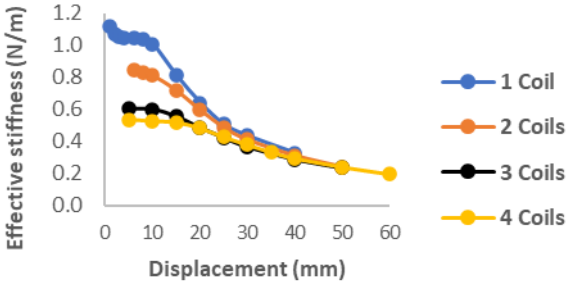

Figure 20 Effective stiffness d 19

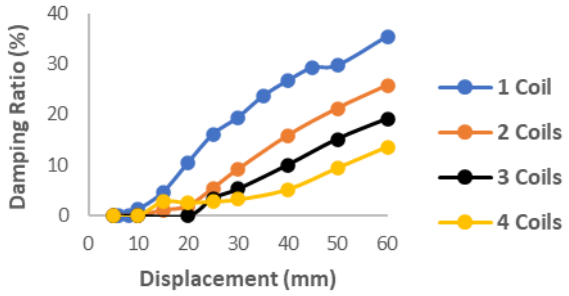

Figure 21 Damping Ratio (EVDR) of helical spring - d 6

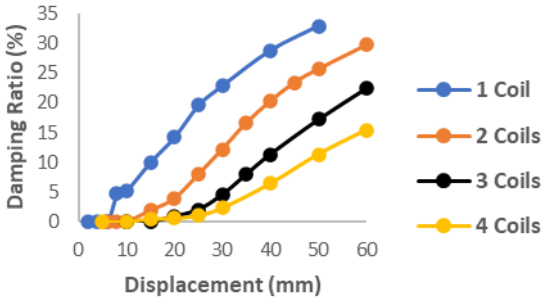

Figure 22 Damping Ratio (EVDR) of helical spring - d 8

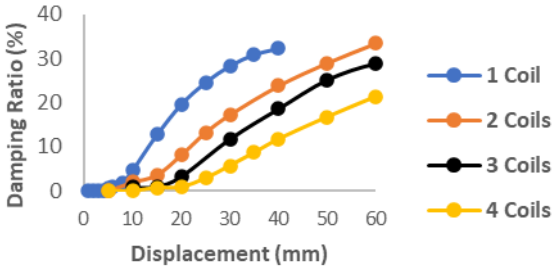

Figure 23. Damping Ratio (EVDR) of helical spring - d 10

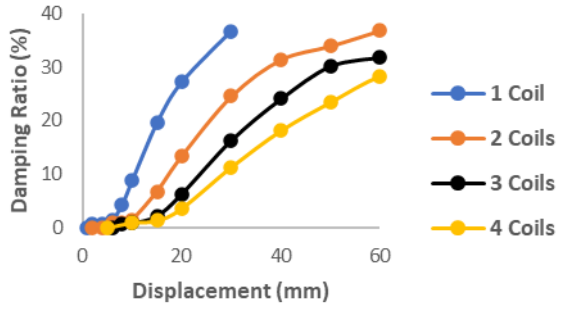

Figure 24 Damping Ratio (EVDR) of helical spring - d 12

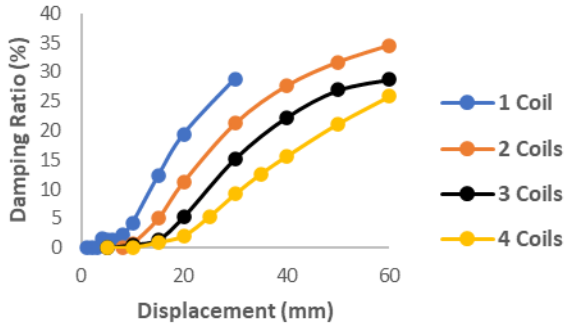

Figure 25 Damping Ratio (EVDR) of helical spring - d 16

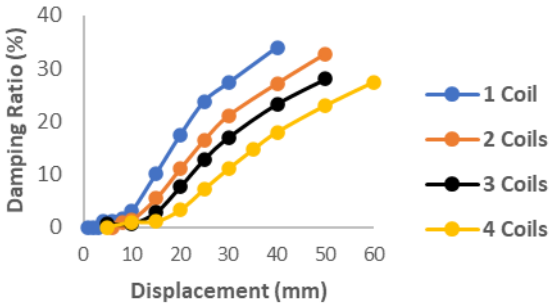

Figure 26 Damping Ratio (EVDR) of helical spring - d 19

Figures 31 to 34 show the differences between the analysis and experiment results for yield displacement. From these figures for specimens with a single coil, the maximum percentage difference between analytical and experimental results at 19 mm diameter was 30%, while the minimum difference at 10 mm diameter was 7%. In the specimen with two coils, the largest difference occurred at 19 mm, with a value of 30%, and the lowest value of 2% was found at 10 mm. In addition, the largest difference at a diameter of 6 mm was 18% for the specimen with three coils, and the smallest difference of 1% was observed 10 mm. The maximum percentage difference between experimental and analytical results for the specimen with four coils was found at 16 mm diameter of 40%, while the minimum difference of 2% occurred at 10 mm. The difference between experimental results and analytical calculations improved with increasing steel bar diameter. As explained in previous studies [22], this could be caused by variations in material characteristics, changes in properties due to the testing process, and manual production methods without adequate supervision. Therefore, mechanical production processes and proper quality control would be required, particularly in manufacturing helical springs with large steel bar diameters.

Table 3 Analytical calculation results of helical spring

No	Steel bars diameter, d (mm)	Coil diameter, D (mm)	n	f_y (MPa)	$C = D/d$	K	τ	F(N)	y(mm)
1	6	85	1	510.79	14.17	1.04	294.91	284.26	13.06
2	6	81	2	510.79	13.50	1.04	294.91	297.80	23.67
3	6	76	3	510.79	12.67	1.04	294.91	316.64	31.19
4	6	71	4	510.79	11.83	1.04	294.91	338.04	36.19
5	8	78	1	496.17	9.75	1.05	286.46	702.40	8.01
6	8	80	2	496.17	10.00	1.05	286.46	685.67	16.87
7	8	79	3	496.17	9.88	1.05	286.46	693.93	24.66
8	8	75	4	496.17	9.38	1.05	286.46	729.07	29.55
9	10	85	1	448.64	8.50	1.06	259.02	1130.19	7.47
10	10	86	2	448.64	8.60	1.06	259.02	1117.77	15.30
11	10	80	3	448.64	8.00	1.06	259.02	1196.67	19.78
12	10	77	4	448.64	7.70	1.06	259.02	1240.45	24.37
13	12	70	1	410.06	5.83	1.09	236.75	2113.85	3.29
14	12	85	2	410.06	7.08	1.07	236.75	1765.41	9.84
15	12	79	3	410.06	6.58	1.08	236.75	1890.03	12.68
16	12	80	4	410.06	6.67	1.08	236.75	1868.05	17.36
17	16	98	1	429.25	6.13	1.08	247.83	3760.67	5.82
18	16	95	2	429.25	5.94	1.08	247.83	3870.20	10.90
19	16	95	3	429.25	5.94	1.08	247.83	3870.20	16.36
20	16	93	4	429.25	5.81	1.09	247.83	3946.84	20.87
21	19	105	1	442.01	5.53	1.09	255.20	6003.32	4.76
22	19	99	2	442.01	5.21	1.10	255.20	6335.30	8.42
23	19	100	3	442.01	5.26	1.10	255.20	6277.45	12.90
24	19	98	4	442.01	5.16	1.10	255.20	6394.24	16.49

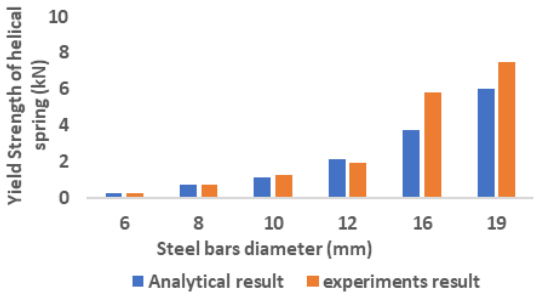

Figure 27 Comparison between analytical and experimental result for the helical spring strength at yielding -Number of coils variations 1

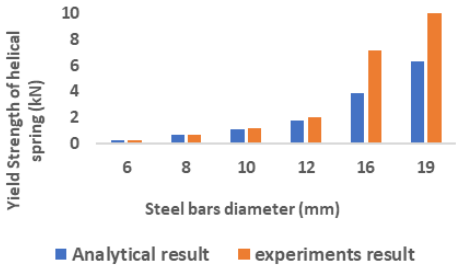

Figure 28 Comparison between analytical and experimental result for the helical spring strength at yielding -Number of coils variations 2

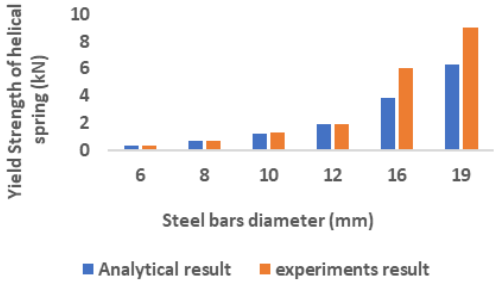

Figure 29 Comparison between analytical and experimental result for the helical spring strength at yielding -Number of coils variations 3

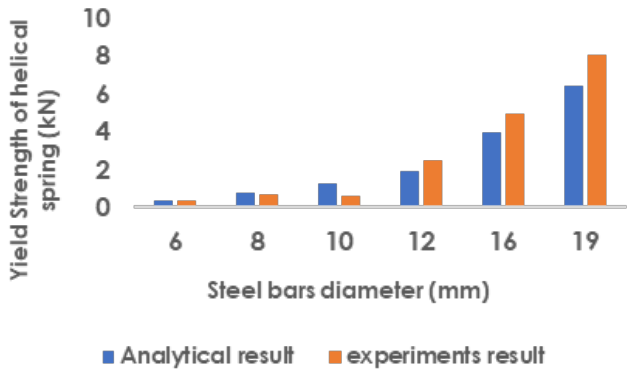

Figure 30 Comparison between analytical and experimental result for the helical spring strength at yielding -Number of coils variations 4

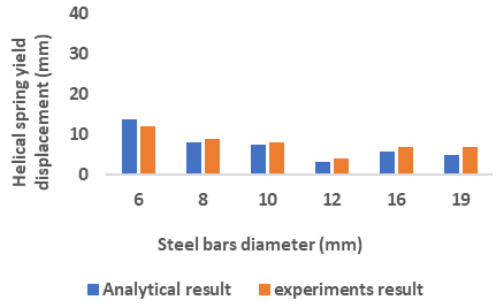

Figure 31 Comparison between analytical and experimental result for the helical spring displacement at yielding -Number of coils variations 1

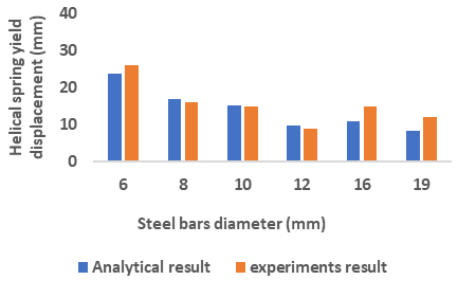

Figure 32 Comparison between analytical and experimental result for the helical spring displacement at yielding -Number of coils variations 2

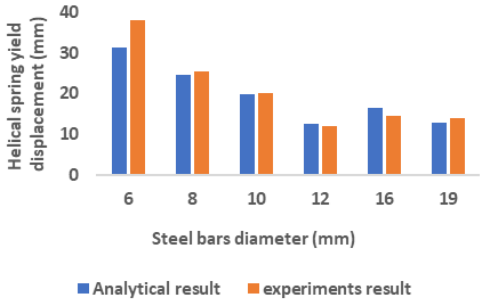

Figure 33 Comparison between analytical and experimental result for the helical spring displacement at yielding -Number of coils variations 3

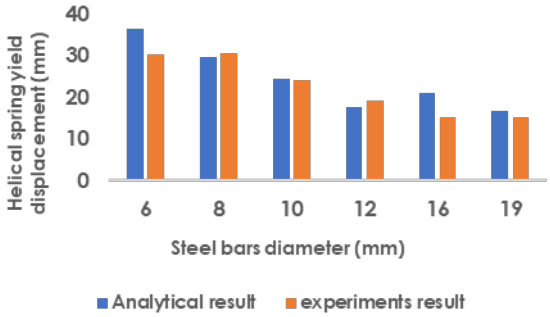

Figure 34 Comparison between analytical and experimental result for the helical spring displacement at yielding -Number of coils variations 4

4.0 CONCLUSION

In conclusion, the study on helical springs showed that increasing the diameter of the helical spring contributed significantly to an increase in the yield strength of the material. The highest yield strength was recorded for the 19 mm diameter steel bar, showing an increase of 96 % compared with the 6 mm specimen. Furthermore, increasing steel bar diameter led to a corresponding increase in the effective stiffness of the helical spring, with the highest stiffness observed in the 19 mm diameter configuration, consistent with its highest yield strength. The damping values for the various helical spring configurations were relatively similar. However, a marked decrease in the damping values was observed as the coil number increased. The highest damping ratios, ranging from 37 to 29%, were observed for the single coil configuration at all steel bar diameters. The differences between experimental results and analytical calculations for steel were attributed to variations in material properties, changes caused by the testing process, as well as manual production methods without quality control. Therefore, mechanical production processes and appropriate quality control were necessary. Future studies should apply helical springs in the structural systems of low-rise lightweight structures, particularly because of the potential for improving energy dissipation, increasing structural resilience, and amending building

performance as well as safety under dynamic loading conditions.

Acknowledgment

This study was funded by the "Hibah PENELITIAN TERAPAN KOMPETITIF NASIONAL (PTKN)".

Conflicts of Interest

The authors declare that there is no conflict of interest regarding the publication of this paper.

References

[1] Katsimpini, Panagiota, G. Papagiannopoulos, and G. Hatzigeorgiou. 2025. A Thorough Examination of Innovative Supplementary Dampers Aimed at Enhancing the Seismic Behavior of Structural Systems. *Applied Sciences.* 15(3): 1226. https://doi.org/10.3390/app15031226.

[2] Pemerintah Indonesia. 2011. *Undang-Undang No. 1 Tahun 2011 tentang Perumahan dan Kawasan Permukiman*. Lembaran Negara Republik Indonesia Tahun 2011 Nomor 7. Jakarta: Sekretariat Negara.

[3] Zhang, Yating, Juan F. Fung, Dustin Cook, Katherine J. Johnson, and Siamak Sattar. 2024. Benefit–Cost Analysis for Earthquake-Resilient Building Design and Retrofit: State of the Art and Future Study Needs. *Natural Hazards Review*. 25(3): 03124001. https://doi.org/10.1061/NHREFO.NHENG-1910.

[4] Buckle, Ian G. 2000. Passive Control of Structures for Seismic Loads. *Bulletin of the New Zealand Society for Earthquake Engineering.* 33(3): 209–221. https://doi.org/10.5459/bnzsee.33.3.209-221.

[5] Setiawan, A. F., Ali. Awaludin, I. Satyarno, N. Md Nor, Y. Haroki, M. F. Darmawan, S. Purnomo, and I. H. Sumartono. 2025. Cyclic Behavior of Multidirectional Box-Shaped Shearing Damper. *Journal of the Civil Engineering Forum*. 11(2): 203-216. https://doi.org/10.22146/jcef.14550

[6] Ampangallo, B. A., H. Parung, R. Irmawaty, and A. Amiruddin. 2024. Effective Stiffness and Damping Analysis of Steel Damper to Lateral Cyclic Loading. *Civil Engineering Journal.* 10(7). http://dx.doi.org/10.28991/CEJ-2024-010-04-019.

[7] Al-Sadoon, Z. A., and M. Almohammad-Albakkar. 2024. Seismic Resilience of Steel-Braced Frames Incorporating Steel Slit Dampers: A Review and Comparative Numerical Analysis. *Civil Engineering Journal.* 10(7). http://dx.doi.org/10.28991/CEJ-2024-010-04-019.

[8] Sahoo, P., B. Majhi, and P. K. Sahu. 2024. "An Experimental Investigation on Tuned Mass Damper for Mitigation of Structural Response of Frame Structures. *Romanian Journal of Acoustics and Vibration*. 21(2): 153–161.

[9] Dirbas, W., A. Diken, and K. Alnefaie. 2025. Enhancement of Wind Turbine Vibrational Behavior by Using a Pendulum Tuned Mass Damper. *Engineering, Technology & Applied Science Research.* 15(3): 22580–22588. https://doi.org/10.48084/etasr.10589.

[10] Xu, K., Q. Li, K. Zhou, and X. Han. 2024. Dynamic Performance of a Supertall Building with an Active Tuned Mass Damper System during Super Typhoon Saola. *Engineering Structures.* 318: 118778. https://doi.org/10.1016/j.engstruct.2024.118778.

[11] Wang, L., Y. Zhou, and Z. Zhou. 2024. Seismic Response Control of Tall Building Using Semi-Active Tuned Mass Damper Considering Soil–Structure Interaction. *Soil Dynamics and Earthquake Engineering.* 187: 108987. https://doi.org/10.1016/j.soildyn.2024.108987.

[12] Naderpour, H., A. SoltaniMatin, A. Kheyroddin, Fakharian, and N. Ezami. 2024. Optimizing Seismic Performance of Tuned Mass Dampers at Various Levels in Reinforced Concrete Buildings. *Buildings.* 14: 2443. https://doi.org/10.3390/buildings14082443.

[13] Nakamura, Y., and R. Matsumura. 2022. Cross-Story Installation of Viscous Dampers in Timber Frame Houses for Earthquake Damage Reduction. *Frontiers in Built Environment.* 8: 1037832. https://doi.org/10.3389/fbuil.2022.1037832.

[14] Cabal, M. R., L. G. Noreña, O. D. Montoya, D. Hincapié, and B. D. Caicedo. 2024. Optimal Design of Helical Spring Using Metaheuristic Techniques. *Mathematical Modelling of Engineering Problems.* 11(10): 2595–2605. https://doi.org/10.18280/mmep.111001.

[15] Kamil, F., A. G. Abdulshaheed, and M. A. Kadhom. 2024. Development of a Computational System to Design a Helical Spring. *International Review of Applied Sciences and Engineering.* 15(3): 287–293. https://doi.org/10.1556/1848.2024.00711.

[16] Zhang, Z., L. He, J. Ni, Z. Cui, J. Sun, and Z. Zhu. 2024. Enhanced Compression Performance of an Improved Rectangular Helical Spring Incorporated Support Feature. *Heliyon.* 10(10): e35102. https://doi.org/10.1016/j.heliyon.2024.e35102.

[17] Bai, B. J., S. L. Li, N. Fantuzzi, and T. W. Liu. 2024. Tensile Performance of 3D-Printed Helical Spring. *Mechanics of Advanced Materials and Structures.* 31(30): 13097–13109. https://doi.org/10.1080/15376494.2024.2332479.

[18] Zhu, J., J. Wang, S. Yang, X. Chen, X. Zhu, Md. S. Fuad, and Y. Qin. 2025. Composite Structure Helical Spring with Designability of Spring Constants: Structural Design and Compression Property Evaluation. *Polymer Composites*. 1–13. https://doi.org/10.1002/pc.29856.

[19] Islam, T., Md. W. Uddin, and R. Uddin. 2024. Finite Element Analysis of Motorcycle Suspension System Stability Using Different Materials. *Journal of Engineering Study*. https://doi.org/10.1016/j.jer.2024.01.020.

[20] Chen, L., J. Chong, Q. Jiang, L. Wu, and Y. Tang. 2024. Understanding the Static Performance of Composite Helical Spring with Braided Nested Structures. *Composites Part A.* 176: 107822. https://doi.org/10.1016/j.compositesa.2023.107822.

[21] Alexandron, and G. deBotton. 2024. Experimental Study of Nitinol Springs: Apparatus and Results. *Experimental Mechanics.* 64: 981–994. https://doi.org/10.1007/s11340-024-01059-9.

[22] Almeida, D., M. Ciaccia, and D. Ojeda. 2024. Mechanical Behavior Characterization of Helical Extension Springs Manufactured in Ecuador. *Applied Engineering and Innovative Technologies*. https://doi.org/10.1007/978-3-031-70760-5_20.

[23] Lv, H., and B. Huang. 2024. Vibration Reduction Performance of a New Tuned Mass Damper with Pre-Strained Superelastic SMA Helical Spring. *International Journal of Structural Stability and Dynamics.* 24(5). https://doi.org/10.1142/S0219455424500470.

[24] Zouatine, M., L. Helm, and H. Sadegh-Azar. 2024. Seismic Performance and Design of an Innovative Structure with Controlled Rocking Shear Wall Using Ring Springs. *Soil Dynamics and Earthquake Engineering.* 185: 108911. https://doi.org/10.1016/j.soildyn.2024.108911.

[25] Budynas, R. G., and J. K. Nisbett. 2014. *Shigley's Mechanical Engineering Design*. New York, NY: McGraw-Hill Education.

[26] Khurmi, R. S., and J. K. Gupta. 2005. *A Textbook of Machine Design*. New Delhi: Chand Publishing.

[27] Tso, W. K., T. J. Zhu, and A. C. Heidebrecht. 1992. Engineering Implication of Ground Motion A/V Ratio. *Soil Dynamics and Earthquake Engineering.* 11 (3): 133–144. https://doi.org/10.1016/0267-7261(92)90027-B.

[28] Park, R. 1989. "Evaluation of Ductility of Structures and Structural Assemblages from Laboratory Testing. *Bulletin of*

the New Zealand National Society for Earthquake Engineering. 22(3): 155–166. https://doi.org/10.5459/bnzsee.22.3.155-166.

[29] Elmenshawi, A., M. Sorour, A. Mufti, L. G. Jaeger, and N. Shrive. 2010. "Damping Mechanisms and Damping Ratios in Vibrating Unreinforced Stone Masonry. *Engineering Structures* 32 (10): 3269–3278.